Journal of Solid State Chemistry 182 (2009) 1907–1912

Contents lists available at ScienceDirect

Journal of Solid State Chemistry

journal homepage: www.elsevier.com/locate/jssc

Deuterium ordering in Laves-phase deuteride $YFe_2D_{4.2}$

J. Ropka [a], R. Černý [a,*], V. Paul-Boncour [b], Th. Proffen [c]

[a] Laboratory of Crystallography, University of Geneva, quai E.-Ansermet 24, CH-1211 Geneva, Switzerland
[b] CMTR, ICMPE, CNRS, 2 rue H. Dunant, 94320 Thiais Cedex, France
[c] Lujan Neutron Scattering Center, LANL, MS H805, Los Alamos, NM 87545, USA

ARTICLE INFO

Article history:
Received 26 February 2009
Received in revised form
24 April 2009
Accepted 28 April 2009
Dedicated to Jim Richardson (IPNS, Argonne)
Available online 9 May 2009

Keywords:
Laves-phase
Deuterium ordering
Powder diffraction

ABSTRACT

The structure of Laves-phase deuteride $YFe_2D_{4.2}$ has been investigated by synchrotron and neutron (*ToF*) powder diffraction experiments between 60 and 370 K. Below 323 K, $YFe_2D_{4.2}$ crystallizes in a fully ordered, monoclinic structure (s.g. *Pc*, $Z=8$, $a=5.50663(4)$, $b=11.4823(1)$, $c=9.42919(6)$ Å, $\beta=122.3314(5)^\circ$, $V=503.765(3)$ Å^3 at 290 K) containing 4 yttrium, 8 iron and 18 deuterium atoms. Most D–D distances are, within the precision of the diffraction experiment, longer than 2.1 Å; the shortest ones are of 1.96 Å. Seven of eight iron atoms are coordinated by deuterium in a trigonal bipyramid, similar to that in $TiFeD_{1.95-2}$. The eighth iron atom is coordinated by deuterium in a tetrahedral configuration. The coordination of iron by deuterium, and the iron-deuterium distances point to the importance of the directional bonding between iron and deuterium atoms. The lowering of crystal symmetry due to deuterium ordering occurs at much higher temperature than the magnetic ordering, and is therefore one of the parameters that are at the origin of the magnetic transition at lower temperatures.

1. Introduction

The deuterides of cubic (C15) Laves-phases AB_2 (*A*—rare earth, *B*—transition metal) have been widely studied for the influence of deuterium absorption on their magnetic properties. YFe_2, which can absorb up to 5 H per formula unit (/f.u.), is particularly interesting owing to the large variety of crystal structures obtained at different hydrogen content [1–7]. These crystal structures are related to an ordering of hydrogen atoms into interstitial sites below an order-disorder temperature T_{OD}, which leads either to superstructures or to a distortion of the cubic C15 structure of the parent intermetallic. Above the ordering temperature, the hydrides preserve the symmetry of the cubic Laves-phase structure with hydrogen distributed on 96*g* (Y_2Fe_2) and 32*e* (Y_1Fe_3) sites. Most ordered crystal structures of the corresponding deuterides, including the position and occupation factor of deuterium atoms, have been characterized [5], with the exception of $YFe_2D_{1.9}$ and $YFe_2D_{4.2}$, which show a low symmetry and very large number of possible hydrogen interstitial sites.

Above the deuterium ordering temperature, $T_{OD}=343$ K, $YFe_2D_{4.2}$ crystallizes in the cubic structure (*Fd*-3*m*, $a=7.95$ Å); between 323 and 343 K it shows a rhombohedral distortion (*R*-3*m*, $a=5.702$ Å, $c=12.404$ Å); and below 323 K down to 2 K it has a monoclinic superstructure [7]. The monoclinic superstructure has been described [8] in s.g. $P2_1/a$ with cell parameters $a=9.399(3)$, $b=5.740(3)$, $c=5.494(3)$ Å, $\beta=122.22(3)^\circ$, which contains 11 partly occupied deuterium sites. Closer examination of the neutron powder patterns showed the existence of additional lines, which could be indexed by doubling the cell parameter *b* as proposed in [8]. This supestructure can be then described in the monoclinic space group *P*1*a*1 (in standard setting *Pc* when interchanging lattice parameters *a* and *c*). However, no attempt has been made to solve the structure in the doubled cell so far, due to the large number of possible interstitial sites for D atoms (64) and, therefore, of atomic positions and occupancy factors to refine (256). A similar monoclinic superstructure was observed at 290 K in the phase of lower deuterium content $YFe_2D_{3.5}$ [9]. This latter phase derives from the same average monoclinic cell with parameters $a=9.482$, $b=5.633$, $c=5.494$ Å, $\beta=123.84^\circ$, keeping the parameters *a* and *b*, while the third parameter is the doubled face diagonal *a*+*c*. The structure was refined in the symmetry $P2_1/a$ resulting in 15 disordered deuterium positions with short D–D contacts.

The YFe_2D_x deuterides are ferromagnets in which the Curie temperature decreases with increasing *x* for $0\le x\le 3.5$ [10]. YFe_2D_5 is a weak ferromagnet, without ordered Fe moments [6]. At the zero-field transition temperature, $T_{MO}=84$ K, $YFe_2D_{4.2}$, the intermediate phase between $3.5<x<5$, undergoes a sharp magnetostrictive transition [7], associated with a transition from a ferromagnetic (F), below $T_{MO,}$ to an antiferromagnetic (AF) structure, above T_{MO}, characterized by a doubling of the magnetic cell along the *b*-axis [8]. The Néel temperature T_N, corresponding

* Corresponding author.
E-mail address: Radovan.Cerny@cryst.unige.ch (R. Černý).

0022-4596/$ - see front matter © 2009 Elsevier Inc. All rights reserved.
doi:10.1016/j.jssc.2009.04.033

to the disappearance of the AF lines in the neutron powder diffraction pattern (NPD), is located at 131 K [7]. Above this temperature the compound is paramagnetic (P). The F–AF magnetic transition is strongly dependent on the applied magnetic field, and presents an itinerant-electron metamagnetic behaviour. A volume decrease of 0.55% was also observed at the transition from the F to the AF state [8]. In addition, a strong magnetic isotope effect is observed for the $YFe_2(D_yH_{1-y})_{4.2}$, as T_{MO} is shifted from 84 K for $y = 0$ to 112 K for $y = 0.64$ and 131 K for $y = 1$ [11]. This isotope effect was partly attributed to the high sensitivity of the magnetic transition to the difference of volume (0.8%) observed between the hydride and the deuteride.

In this paper we will give the complete description of the monoclinic crystal structure of $YFe_2D_{4.2}$ between 290 and 60 K. The localization of the D atoms is particularly important to analyze the Fe atom environments and to understand more clearly the origin of the F–AF transition, and the associated strong isotope effect. The magnetic structure of the AF phase, and the local order of deuterium atoms around the iron, studied by the Pair Distribution Function analysis of the diffuse intensity of the neutron powder pattern, will be communicated separately.

2. Experimental

The YFe_2 intermetallic compound was prepared by induction melting of the pure elements followed by three weeks of annealing at 1100 K. The composition and homogeneity was checked by X-ray powder diffraction (XPD) and electron probe microanalysis (EPMA) as described in [7]. The $YFe_2D_{4.2}$ deuteride was prepared by solid–gas reaction using a Sievert apparatus and its homogeneity was checked by XPD. Two samples were independently prepared by this protocol and will be called sample nos. 1 and 2.

X-ray powder diffraction measurements were carried out using a Bruker D8 diffractometer (Cu$K\alpha$ radiation). Several synchrotron powder patterns (SPD) were collected on the sample no. 2 at the Swiss–Norwegian Beam Line BM1B of the ESRF, Grenoble, France, to follow the temperature dependence of lattice parameters. The powder sample was closed in a 0.5 mm glass capillary, and the temperature was controlled with a special He-cryostat. Diffraction patterns ($\lambda = 0.40001$ Å) were collected with a 6-crystal analyzer detector.

The time-of-flight (*ToF*) neutron powder data were collected at the GPPD spectrometer at the IPNS, Argonne National Laboratory (sample 1, $T = 290$, 350 and 370 K), and at the NPDF spectrometer at the LANSCE, Los Alamos National Laboratory (sample 2, $T = 60$, 96, 200, 290 K), USA. The sample (7.7 g of sample no. 1, and 4.8 g of sample no. 2) was closed in a vanadium container, and the temperature was controlled by the Displex attachment.

The crystal structure was solved by the global optimization of the positions of deuterium atoms in the elementary cell (*Pc*) with the help of the program Fox [12]. The profile matching using the synchrotron data was done with the program FullProf [13]. The Rietveld refinement using the *ToF* data was done with the program GSAS [14].

3. Results

3.1. Lattice

The monoclinic *Pc* phase is observed at temperatures below 290 K, in agreement with [7]. The variation of the volume/8 f.u. of $YFe_2D_{4.2}$ (= monoclinic cell volume) with the temperature as obtained on both samples and from different diffraction

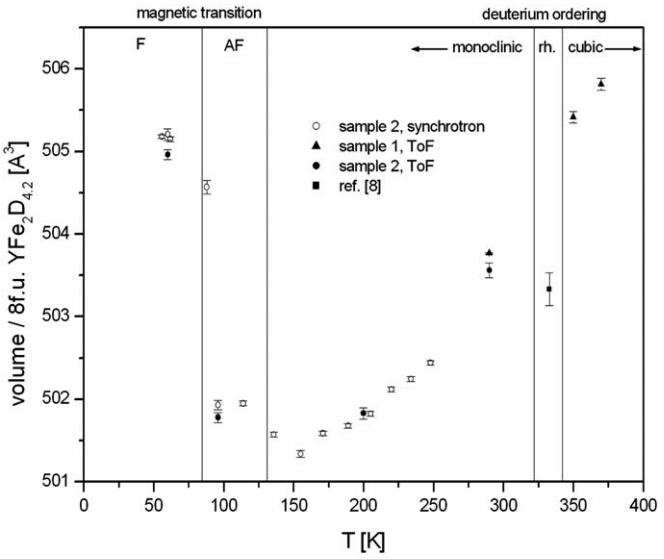

Fig. 1. Temperature dependence of the volume/8 f.u. $YFe_2D_{4.2}$ (= monoclinic cell volume) from different powder diffraction experiments. A decrease of 0.653% is observed at the transition from ferromagnetic (F) to antiferromagnetic (AF) phase. Similar volume increase is observed at the transition from ordered monoclinic to disordered cubic phase separated by the region of the rhombohedrally distorted phase (rh) as observed in [8].

experiments is given in Fig. 1. It shows the effect of the magnetic phase transition at $T_{MO} = 84$ K and of deuterium ordering at $T_{OD} = 343$ K. A sharp volume increase is observed at the AF to F transition. The volume is also bigger in the deuterium-disordered cubic phase as compared to the P monoclinic phase. Variation of monoclinic lattice parameters with temperature is given in Fig. 2. The "monoclinic" lattice parameters at 350 and 370 K were calculated from the cubic lattice of the disordered $YFe_2D_{4.2}$ phase according to Eq. 1 given in the Dicussion. In a similar way the volume/8 f.u. of $YFe_2D_{4.2}$, and "monoclinic" lattice parameters of the rhombohedral phase at 333 K were calculated from the reported data [8], and are shown in the Figs. 1 and 2 too. In agreement with [7] the monoclinic lattice parameters show strong anisotropy (*b*-parameter increases) of the lattice contraction at deuterium ordering and a weak anisotropy (all parameters increase) of the lattice expansion, due to the magnetoelastic effect at the transition from AF to F magnetic order. The volume increase between 96 and 60 K as observed on sample no. 2 is 0.653%. The magnetoelastic effect is less pronounced along the *b*-axis. The thermal dilatation is also strongly anisotropic, weaker along the *b*-axis, and stronger along the *a*-and *c*-axes, and shows an anomaly when approaching the magnetic phase transition temperature T_{MO}.

3.2. Structure

When solving the crystal structure from *ToF* neutron data we have used the 290 K data of sample no. 1. The positions of the metal atoms of $YFe_2D_{4.2}$ as described in the space group $P2_1/a$ [8] were transformed to the space group $P1a1$ with doubled cell volume ($b_{Pa} = 2b_{P21/a}$). This model, with the positions of the metal atoms fixed, was used as a starting configuration for the localization of deuterium atoms using neutron data measured at 290 K, where no contribution of magnetic peaks is observed. For the Rietveld refinement using the data at 96 and 60 K we have excluded the strongest magnetic peaks in the spectra ($d = 4.63$ Å for F ordering, and $d = 23.5$, 5.51 and 3.98 Å for AF ordering). The

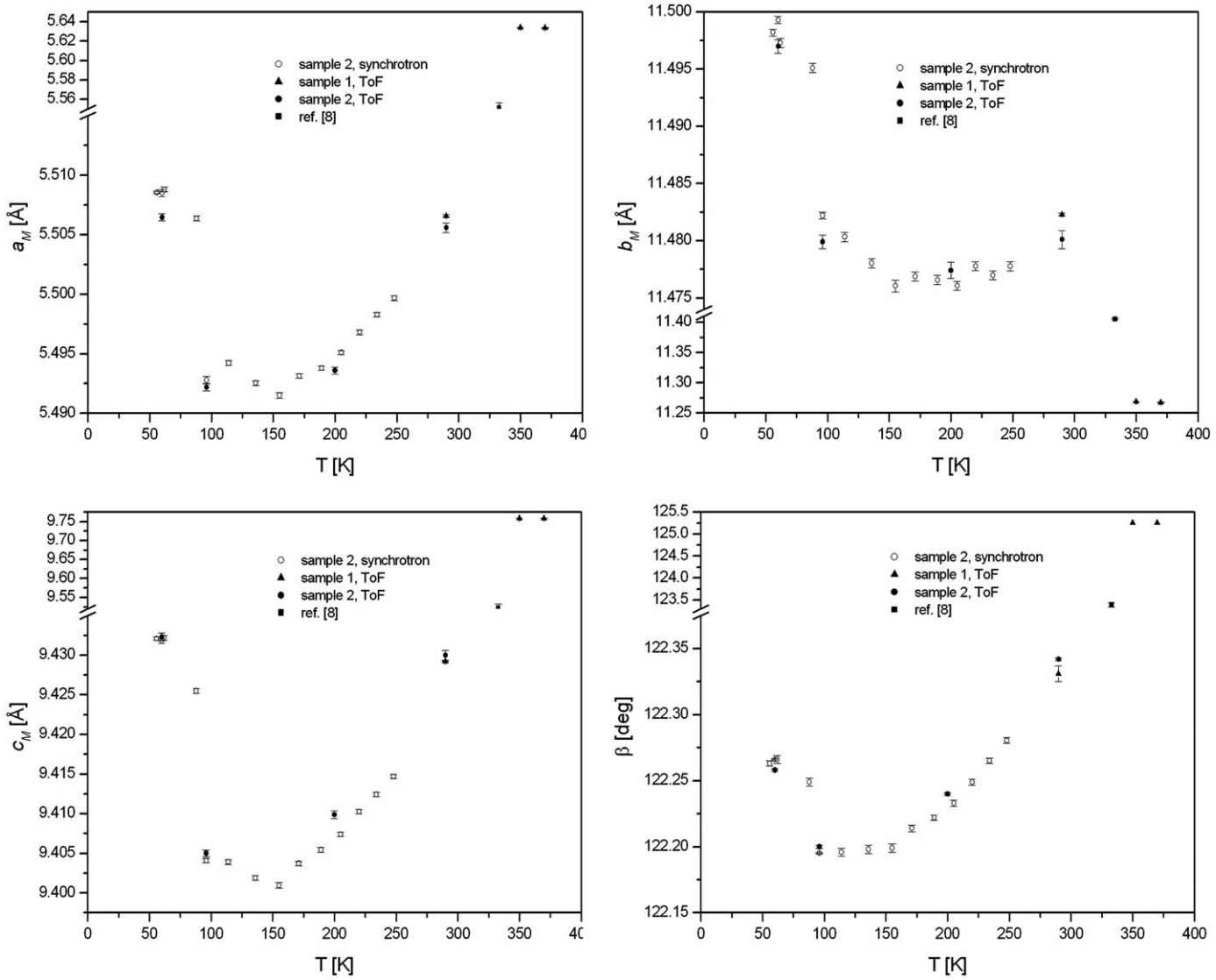

Fig. 2. Temperature dependence of the monoclinic lattice parameters of $YFe_2D_{4.2}$ from different powder diffraction experiments showing strong anisotropy (*b*-parameter increases) of the lattice contraction at deuterium ordering and a weak anisotropy (all parameters increase) of the lattice expansion at the transition from AF to F magnetic order. The ''monoclinic'' lattice parameters at 333, 350 and 370 K are calculated by the transformation from the rhombohedral and cubic lattices.

contribution of other magnetic peaks was checked by comparing the data below and above $T_N = 131$ K, and was found negligible. The $YFe_2D_{4.2}$ structure was finally solved in the space group *P*1*c*1 with 12 independent metal atoms (Y on four sites 2*a* and Fe on eight sites 2*a*), and 18 deuterium atoms on sites 2*a*. The atomic parameters at 290 K refined on sample no. 1 are given in Supporting Information (Table S1a). The displacement parameters were constrained to be identical for all atoms of same type, to minimize the correlation between the displacement parameter and occupancy of deuterium site. The coordination of yttrium and iron atoms by deuterium atoms is given in Table S2. The refined composition is $YFe_2D_{4.27(5)}$. Traces of disordered cubic phase with lattice parameter $a = 7.9198(1)$ Å, and refined composition $YFe_2D_{4.54(4)}$, were observed in the *ToF* data at 290 K. Its weight fraction, as refined from the Rietveld refinement, was 4.0(1)%.

The Rietveld refinement of the disordered phase at 350 and 370 K showed the cubic structure of the Laves-phase deuteride with the 96*g* site preferentially occupied by deuterium, the 32*e* site less occupied, and the 8*b* site nearly empty, in agreement with [8]. Further heating of the sample to 400 K resulted in a partial desorption of deuterium and decrease of the cell volume and refined deuterium content. The atomic parameters at 350 K refined on sample no. 1 are given in the Supporting Information (Table S1b). The refined deuterium content $YFe_2D_{4.65(2)}$ is higher than that of the ordered monoclinic phase at 290 K. The refinement agreement factors, especially R_{Bragg}, are also higher compared to the refinement at 290 K. The same discrepancy was observed also at 370 K. The discrepancy between the refined deuterium content in the same sample in the ordered and disordered states can be understood as a result of the diffuse intensity of the disordered phase, which is ignored in the Rietveld refinement. Very strong diffuse intensity, due to short-range D–D correlations, is observed in all neutron powder patterns of $YFe_2D_{4.2}$ in the disordered state. As Rietveld refinement ignores this observation, it results in a wrong estimation of the deuterium content in the sample, in our case to its overestimation, and to higher agreement factors. The same overestimation of the deuterium content by the Rietveld refinement was observed in the rhombohedral phase [8], which is not fully ordered, and shows a similar preference for the site occupation by deuterium to the cubic phase with even stronger preference for the three available Y_2Fe_2 sites to two Y_1Fe_3 sites.

Table 1
First neighbors interatomic distances (Å) and deuterium coordination if iron atoms in $YFe_2D_{4.2}$ as refined from the neutron *ToF* data as a function of the temperature, sample no. 2.

Temperature (K)	290	200	96	60
Fe–D				
max	1.84	1.90	1.83	1.84
min	1.62	1.58	1.62	1.61
av	1.72	1.72	1.72	1.73
CN Fe1	**3.82**	**3.61**	**3.81**	**3.84**
CN Fe6	**4.36**	**4.38**	**4.53**	**4.42**
CN Fe8	**4.32**	**4.54**	**4.47**	**4.40**
CN Fe (without Fe6,Fe8)	**4.67**	**4.71**	**4.76**	**4.80**
Y–D				
max	2.62	2.43	2.43	2.43
min	2.12	2.13	2.14	2.13
av	2.25	2.25	2.24	2.25
Fe–Fe				
max	3.00	3.00	2.98	3.00
min	2.67	2.71	2.67	2.68
av	2.81	2.81	2.81	2.82
Y–Y				
max	3.56	3.49	3.49	3.51
min	3.36	3.37	3.37	3.38
av	3.45	3.44	3.44	3.45

The structural model obtained from sample no.1 at 290 K was used for the refinement using the temperature-dependent *ToF* data from sample no. 2. The same atomic parameters as for the sample no. 1 were refined giving at 290 K identical results within the obtained precision. The *ToF* data measured on sample no. 2 at 200, 96 and 60 K do not show any structural transition or modification, and the structural model stays in principle identical as at 290 K (see essential interatomic distances and coordination in Table 1).

The Rietveld plot of three data banks at 290 K from the GPPD diffractometer are shown in the Figure S1, and of three data banks at 96 K from the NPDF diffractometer are shown in the Figure S2 of the Supporting Information. The Crystallographic information files (CIF) of all refined structures are included too.

4. Discussion

4.1. Symmetry of the monoclinic phase

$YFe_2D_{4.2}$ at 290 K is an ordered phase in the monoclinic cell (s.g. *Pc*, $Z=8$, $a=5.50663(4)$, $b=11.4823(1)$, $c=9.42919(6)$ Å, $\beta=122.3314(5)^\circ$, $V=503.765(3)$ Å^3). A relation between the lattice vectors of the cubic disordered and monoclinic ordered $YFe_2D_{4.2}$ is

$$\vec{a}_M \approx \tfrac{1}{2}(\vec{a}_C + \vec{b}_C)$$

$$\vec{b}_M \approx (\vec{a}_C - \vec{b}_C)$$

$$\vec{c}_M \approx -\tfrac{1}{2}(\vec{a}_C + \vec{b}_C + 2\vec{c}_C) \quad (1)$$

where $\vec{a}_M$, $\vec{b}_M$, $\vec{c}_M$ are lattice vectors of the ordered monoclinic and $\vec{a}_C$, $\vec{b}_C$, $\vec{c}_C$ of the disordered cubic phase. The group–subgroup relation between the space group of the disordered phase *Fd*-3*m* and ordered phase *Pc* was analyzed with the help of the program SUBGROUPGRAPH [15]. The index of transformation is 96 and there exist a great number of possible chains between both space groups. However, taking into account that $YFe_2D_{4.2}$ structure is cubic in the disordered state at high temperature, and changes its symmetry through the rhombohedral to the monoclinic phases [7] as temperature decreases, and assuming a group-subgroup relation between the three phases, only one chain of group-subgroup relations can be selected (Fig. 5).

4.2. Atomic coordination

At 290 K all D–D distances are, within the precision of the diffraction experiment, longer than 2.1 Å, except D4–D11 (1.96 Å). If all deuterium sites were fully occupied the composition would be $YFe_2D_{4.5}$. It is worth to note that both samples were not fully saturated, but the refined composition of both samples was close to $YFe_2D_{4.2}$, and it justifies calling the phase by this formula. Of 18 independent deuterium sites, 15 correspond to the 96*g* site (Y_2Fe_2) in the cubic space group *Fd*-3*m* of the disordered phase, and 3 to the 32*e* site (Y_1Fe_3). An interesting feature of the structure is the coordination of the iron atoms by deuterium (Table S2). Seven iron atoms are coordinated by a trigonal bipyramid, in which the angle D–Fe–D for two apical deuterium atoms is in the range 166.1(4)–178.1(4)°, and the angle D–Fe–D for two equatorial deuterium atoms is in the range 102.2(3)–147.5(4)°. Atom Fe1 is coordinated by a tetrahedron with tetrahedral angles within 100.9(3)–122.0(5)°. The ratio between occupied Y_2Fe_2 and Y_1Fe_3 sites in the coordination sphere of iron atoms coordinated by the trigonal pyramid is 4:1 while this ratio is 2:2 for Fe1. The Fe–D distances lie within the range 1.618(7)–1.875(8) Å, and the shortest ones are close to the Fe–D distances of 1.556 Å in Mg_2FeD_6 [16], which contains octahedral 18-electron complexes of $[FeD_6]^{-4}$. It points to the importance of the directional bonding between iron and deuterium atoms in $YFe_2D_{4.2}$. The increased importance of Fe–D bonding in $YFe_2D_{4.2}$ compared to less-deuterium-rich deuterides of YFe_2 was shown in [17]. However, the coordination polyhedra FeD_x in $YFe_2D_{4.2}$ share all D-vertices and cannot be considered as 18-electron complexes. No FeD_5 or FeD_4 complexes are reported so far, and no ionic limiting formula can be written for $YFe_2D_{4.2}$.

Alternative description of the structure of Laves-phase deuterides AB_2D_x as done by analyzing the *A*-atom coordination by deuterium was elaborated in [18]. Three yttrium atoms in the monoclinic $YFe_2D_{4.2}$ are coordinated by 8 and one (Y3) by 9 deuteriums forming irregular polyhedra with Y–D distances lying within the range 2.07(1)–2.47(1) Å. We prefer, however, the FeD_x polyhedral description of the structure in the following discussion. Our preference is justified by the importance of Fe–D over Y–D bonding for stabilizing the monoclinic structure as shown in [17].

Similar trigonal bipyramidal coordination of iron by deuterium, also sharing all vertices, was found in monoclinic $TiFeD_2$ [19] and orthorhombic $TiFeD_{1.95}$ [20]. The Fe–D distances lie within 1.65(1)–1.97(1), slightly longer than in $YFe_2D_{4.2}$. The angle D–Fe–D for two apical deuterium atoms is in the range 164.4(7)–167.0(7)°, and the angle D–Fe–D for two equatorial deuterium atoms is in the range 92.2(1)–133.1(1)°, showing a slightly more deformed trigonal bipyramid in $TiFeD_{1.95-2}$. In contrast to $YFe_2D_{4.2}$, the interstitial sites in $TiFeD_{1.95-2}$ that are occupied by deuterium are octahedral sites of the composition either Ti_2Fe_4 or Ti_4Fe_2.

The question whether the same order of deuterium around the iron atoms also exists locally in the disordered phase $YFe_2D_{4.2}$ above $T_{OD}=343$ K will be treated in a separate paper.

4.3. Deuterium ordering vs. magnetic order

Band structure calculations on YFe_2H_x have shown that the increase of the cell volume due to increasing hydrogen content

stabilizes the ferromagnetic structure with an increase of the Fe moment, whereas the increase of the number of Fe–H bonds tends to reduce the Fe moment until the compound becomes paramagnetic in YFe_2H_5 [21,22]. The magnetic properties of the YFe_2 hydrides (deuterides) result therefore from a competition between volume and electronic change induced by the insertion of H(D) atoms. The AF state of $YFe_2H_{4.2}$ between $T_{MO} = 84$ K and $T_N = 131$ K has been related [11] to the behaviour of the magnetic moment of one iron atom coordinated by more deuterium atoms than other iron atoms. Our results do not show such coordination about an iron atom between 60 and 290 K. In the average structural model of the monoclinic phase in $P2_1/a$ [8] such an iron atom was observed as coordinated by ~5 D atoms contrary to all other iron atoms coordinated by ~4 D atoms. It turned out that this model was only a projection of the true *Pc* model to a cell of half volume.

As shown in the left part of Fig. 3, the structure of the monoclinic $YFe_2D_{4.2}$ can be built up from the $(20\bar{1})$ layers containing Fe2–Fe7D_5 trigonal bypiramids. The layers are then stacked in the direction $[\bar{1}01]$ and connected by Fe1D_4 tetrahedron and Fe8D_5 trigonal bipyramid as shown in Fig. 4. These layers are equivalent to {111} layers of the disordered cubic structure of the Laves-phase deuteride (Fig. 3, right). This description follows the lowering of the symmetry in the cubic-rhombohedral-monoclinic transition on cooling, as the cubic {111} planes become the basal planes {001} of the hexagonal lattice of the rhombohedral phase. On full ordering of deuterium atoms below 323 K in the monoclinic phase, these planes lose the hexagonal symmetry, expand along the b_M direction, and contract along the perpendicular direction. The thermal dilatation observed in the monoclinic phase is weaker within the $(20\bar{1})$ layers (along the *b*-axis) and stronger in the direction perpendicular to the layers (along the *a*+*c* direction) Fig. 2.

Another feature of this description is the particular position of Fe1, Fe6 and Fe8 atoms, which are less (Fe1) or slightly less (Fe6 and Fe8) coordinated by deuterium than are all remaining iron atoms (Table 1). Moreover, Fe1 shows different shape of the coordination polyhedron, and different ratio between occupied Y_2Fe_2 and Y_1Fe_3 sites in the coordination sphere compared to all other iron atoms. The position of Fe6 in the layer may be at the origin of the doubling of the AF cell in the *b*-direction. However, the origin of the observed AF order remains to be understood. Band structure calculations will be performed, using the results of the present work, in order to get a better understanding of the influence of the structural distortion and of the Fe–D bonding on the magnetic properties. We can now only conclude that the lowering of crystal symmetry from cubic over rhombohedral down to monoclinic due to deuterium ordering occurs at much higher temperatures than the magnetic ordering, and is therefore one of the parameters that are at the origin of magnetic ordering.

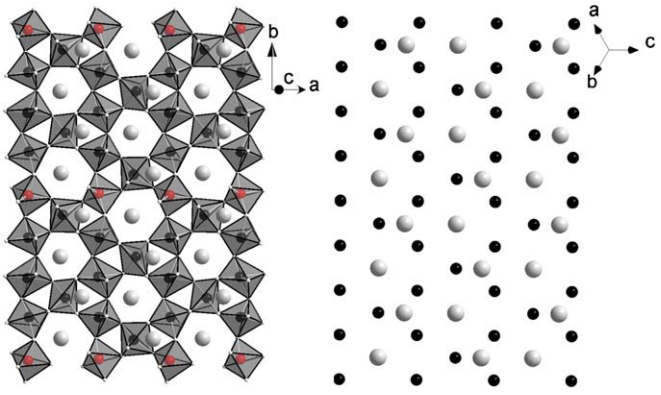

Fig. 3. One $(20\bar{1})$ layer of the monoclinic $YFe_2D_{4.2}$ (left) equivalent to the close packed planes {111} of the cubic structure (right, only metal atoms are shown, Y light, Fe dark), as a basic building unit of the monoclinic structure, built up from Fe2–Fe7D_5 trigonal bipyramids and viewed along $[\bar{1}01]$, Fe6 in red. (For interpretation of the references to color in this figure-legend, the reader is referred to the web version of this article).

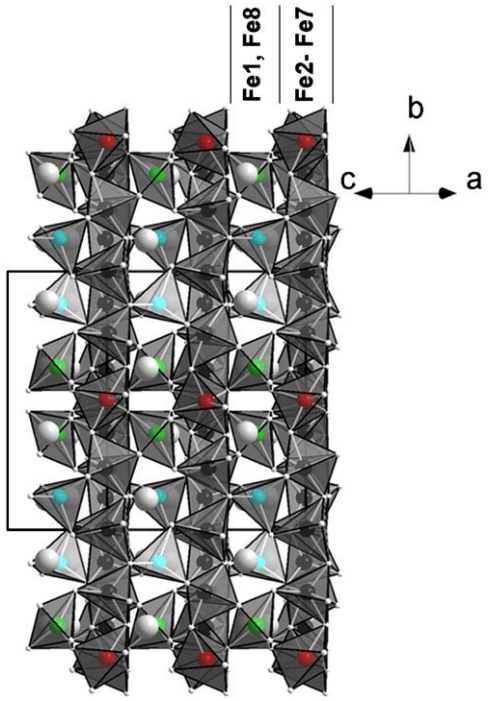

Fig. 4. Structure of the monoclinic $YFe_2D_{4.2}$ as built up from the $(20\bar{1})$ layers (3 layers are shown) viewed along [201]. The layers are connected in the $[\bar{1}01]$ direction by Fe1D_4 tetrahedra and Fe8D_5 trigonal bipyramids, Fe1 in blue, Fe6 in red, Fe8 in green. (For interpretation of the references to color in this figure legend, the reader is referred to the web version of this article).

4.4. Relation to other ordered deuterides of cubic Laves-phases

Other known deuterides of cubic Laves-phases with fully ordered deuterium distribution are monoclinic $ZrCr_2D_4$ [23] below 250 K, orthorhombic ZrV_2D_6 [24] below 210 K, and cubic YMn_2D_6 [25]. Especially the comparison with $ZrCr_2D_4$ is interesting as both structures, $YFe_2D_{4.2}$ and $ZrCr_2D_4$, have monoclinic symmetry with the same direction of the monoclinic axis with respect to the cubic cell of the disordered phase (Eq. 1). Contrary to $YFe_2D_{4.2}$, the interstitial sites occupied by deuterium are all of the 96*g* type (Zr_2Cr_2), and three independent chromium atoms are coordinated by 4 deuteriums in three different configurations. On the other side, the interstitial sites occupied by deuterium in ZrV_2D_6 (if we neglect 6 other nearly empty sites) are of the 96*g* (Zr_2V_2) and 32*e* type (Zr_1V_3) in the ratio 1:1. Two independent vanadium atoms are coordinated by 8 and 7 deuteriums, respectively.

YMn_2D_6 is a special case, as it is probably the true complex deuteride with $[MnD_6]^{5-}$ anionic complexes. It was proposed in [25] that the compound contains Mn in two oxidation states: Mn^{I} in the anionic complex and Mn^{II} on the mixed site with Y^{III}. This hypothesis, however, stays to be confirmed.

We can then conclude that the description of fully ordered deuterides of cubic Laves-phases by BD_x polyhedra seems to be

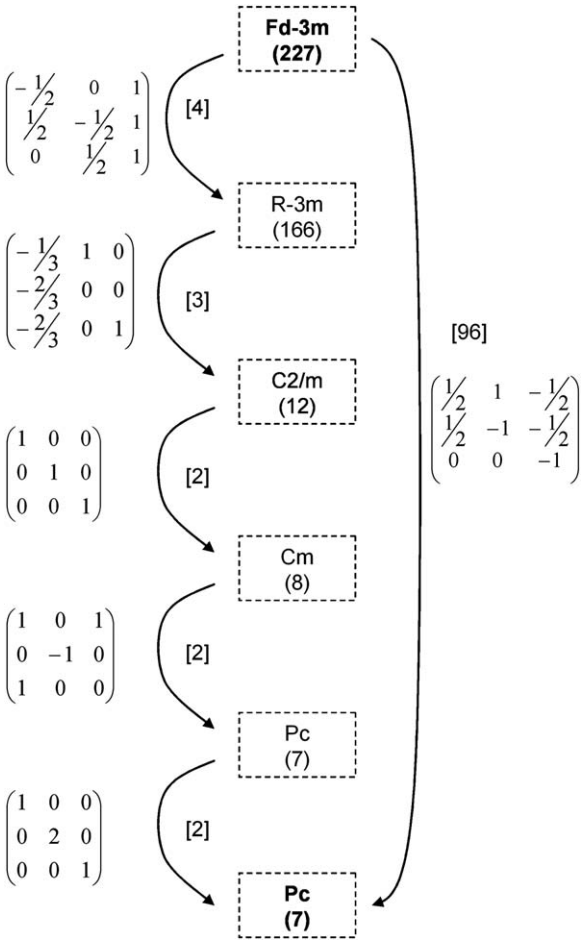

Fig. 5. Chain of group–subgroup relations between the space group of the disordered phase *Fd*-3*m* and ordered phase *Pc* of $YFe_2D_{4.2}$. The transformation matrices between basic lattice vectors and indices of transformations (square brackets) are given.

more appropriate for transition metals *B* containing more bonding 3*d*-electrons like Fe and Mn rather than for Cr or V.

The monoclinic superstructure of the less-deuterium-rich phase $YFe_2D_{3.5}$ [9] is not fully ordered, and cannot therefore be easily related to the fully ordered $YFe_2D_{4.2}$. Both superstructures are created by doubling the periodicity of the common monoclinic sub-cell, but in different directions. The volume/f.u. is smaller in $YFe_2D_{3.5}$ (60.9 Å^3) than in $YFe_2D_{4.2}$ (62.9 Å^3), as expected from the lower deuterium content. The cell expansion due to deuterium content is, however, anisotropic: the parameter *a* (in the common monoclinic sub-cell) is longer in $YFe_2D_{3.5}$ (9.482 Å) than in $YFe_2D_{4.2}$ (9.429 Å). Whether $YFe_2D_{3.5}$ becomes fully ordered at lower temperatures, remains to be investigated.

5. Conclusions

The deuterium atoms in $YFe_2D_{4.2}$ are fully ordered from 290 down to 2 K in the monoclinic cell (s.g. *Pc*, $a = 5.50663(4)$, $b = 11.4823(1)$, $c = 9.42919(6)$ Å, $\beta = 122.3314(5)^\circ$, $V = 503.765(3)$ Å^3 at 290 K). The structural refinement shows that ten of eighteen deuterium sites are partly occupied; however, their occupancies are close to 90%. The saturated deuteride, with all sites fully occupied, would reach the composition $YFe_2D_{4.5}$. The D atoms occupy 15 Y_2Fe_2 and 3 Y_1Fe_3 sites. Most of the D–D distances are longer than 2.1 Å, the shortest one is of 1.96 Å. Seven Fe atoms are coordinated by deuterium in a trigonal bipyramid, similar to that in $TiFeD_{1.95-2}$, whereas the eighth one is coordinated in a tetrahedral configuration. The same structure is maintained at 200, 96 and 60 K. A jump of the cell volume is observed at the AF–F transition. The deuterium ordering, which occurs at much higher temperature than magnetic order, is one of the parameters, which are at the origin of AF and F ordering at lower temperatures.

Acknowledgments

We would like to thank to Hyunjeong Kim (Lujan Center) for the help with ToF data collection, and to Herman Emmerich (SNBL, ESRF Grenoble) for the help with the synchrotron data collection. The help of Yaroslav Tokaychuk (University of Geneva) with the sample synthesis is highly appreciated. This work has benefited from the use of NPDF at the Lujan Center at Los Alamos Neutron Science Center, funded by DOE Office of Basic Energy Sciences. Los Alamos National Laboratory is operated by Los Alamos National Security LLC under DOE Contract DE-AC52-06NA25396. The upgrade of NPDF has been funded by NSF through grant DMR 00-76488. This work was supported by the Swiss National Science Foundation.

Appendix A. Supplementary material

Supplementary data associated with this article can be found in the online version at doi:10.1016/j.jssc.2009.04.033.

References

[1] K.H.J. Buschow, A.M. Van Diepen, Solid State Commun. 19 (1) (1976) 79–81.
[2] V.V. Burnasheva, E.E. Fokina, S.L. Troitskaya, K.N. Semenenko, Russ. J. Inorg. Chem. 29 (6) (1984) 792–794.
[3] K. Kanematsu, J. Appl. Phys. 75 (10) (1994) 7105–7107.
[4] K. Kanematsu, N. Ohkubo, K. Itoh, S. Ban, T. Miyajima, Y. Yamaguchi, J. Phys. Soc. Jap. 65 (4) (1996) 1072–1076.
[5] V. Paul-Boncour, L. Guénée, M. Latroche, A. Percheron-Guégan, B. Ouladdiaf, F. Bourée-Vigneron, J. Solid State Chem. 142 (1999) 120–129.
[6] V. Paul-Boncour, S.M. Filipek, A. Percheron-Guégan, I. Marchuk, J. Pielaszek, J. Alloys Compd. 317–318 (2001) 83–87.
[7] V. Paul-Boncour, G. André, F. Bourée, M. Guillot, G. Wiesinger, A. Percheron-Guégan, Phys. B 350 (2004) e27–e30.
[8] V. Paul-Boncour, M. Guillot, G. André, F. Bourée, G. Wiesinger, A. Percheron-Guégan, J. Alloys Compd. 404–406 (2005) 355–359.
[9] G. Wiesinger, V. Paul-Boncour, S.M. Filipek, Ch. Reichl, I. Marchuk, A. Percheron-Guégan, J. Phys. Condens. Matter 17 (2005) 893–908.
[10] V. Paul-Boncour, A. Percheron-Guégan, J. Alloys Compd. 293–295 (1999) 237–242.
[11] V. Paul-Boncour, M. Guillot, G. Wiesinger, G. André, Phys. Rev. B 72 (2005) 174430.
[12] V. Favre-Nicolin, R. Černý, J. Appl. Cryst. 35 (2002) 734–743.
[13] J. Rodriguez-Carvajal, Phys. B 192 (1993) 55 Remarks: for a more recent version see Rodríguez-Carvajal, J. Recent Developments of the Program FULLPROF, in Commission on Powder Diffraction (IUCr).Newsletter (2001), 26, 12–19. 〈http://journals.iucr.org/iucr-top/comm/cpd/Newsletters/〉 The complete program and documentation can be obtained at 〈http://www.ill.fr/dif/Soft/fp/〉.
[14] A.C. Larson, R.B. Von Dreele, General structure analysis system (GSAS), Los Alamos National Laboratory Report LAUR 86–748, 2004.
[15] S. Ivantchev, E. Kroumova, G. Madariaga, J.M. Perez-Mato, M.I. Aroyo, J. Appl. Cryst. 33 (2000) 1190–1191.
[16] J.-J. Didisheim, P. Zolliker, K. Yvon, P. Fischer, J. Scheffer, M. Gubelmann, A.F. Williams, Inorg. Chem. 23 (1984) 1953–1957.
[17] V. Paul-Boncour, S.F. Matar, Phys. Rev. B 70 (2004) 184435.
[18] A.B. Riabov, V.A. Yartys, J. Alloys Compd. 330–332 (2002) 234–240.
[19] W. Schaefer, G. Will, T. Schober, Mater. Res. Bull. 15 (1980) 627–634.
[20] P. Fischer, J. Schefer, K. Yvon, L. Schlapbach, T. Riesterer, J. Less-Common Met. 129 (1987) 39–45.
[21] D.J. Singh, M. Gupta, Phys. Rev. B. 69 (2004) 132403.
[22] J.C. Crivello, M. Gupta, J. Alloys Compd. 404–406 (2005) 150–154.
[23] H. Kohlmann, F. Fauth, K. Yvon, J. Alloys Compd. 285 (1999) 204–211.
[24] A.N. Bogdanova, A.V. Irodova, G. Andre, F. Bouree, J. Alloys Compd. 356–357 (2003) 50–53.
[25] V. Paul-Boncour, S.M. Filipek, M. Dorogova, F. Bourée, G. André, I. Marchuk, A. Percheron-Guégan, R.S. Liu, J. Solid State Chem. 178 (2005) 356–362.